Proceedings of the ASME 2013 32nd International Conference on Ocean, Offshore and Arctic Engineering
OMAE2013
June 9-14, 2013, Nantes, France

OMAE2013-10984

USING MODEL TEST DATA TO ASSESS VIV FACTOR OF SAFETY FOR SCR AND TTR IN GOM

E.R. Fontaine
AMOG Consulting
Melbourne, Victoria, Australia

J. Rosen
AMOG Consulting
Melbourne, Victoria, Australia

H. Marcollo
AMOG Consulting
Melbourne, Victoria, Australia

J.K. Vandiver
M.I.T.
Cambridge, MA, USA

M. Triantafyllou
M.I.T.
Cambridge, MA, USA

T.L. Resvanis
M.I.T.
Cambridge, MA, USA

C.M. Larsen
NTNU
Trondheim, Norway

M.A. Tognarelli
BP America Production Co.
Houston, TX, USA

O.H. Oakley
Chevron
San Ramon, CA, USA

Y. Constantinides
Chevron
Houston, TX, USA

D.R. Johnstone
AMOG Consulting
Melbourne, Victoria, Australia

ABSTRACT

This paper presents results obtained as part of the DeepStar Phase 10 program on VIV Factors of Safety. The objective was to develop a general methodology to calibrate Factors of Safety for VIV-induced fatigue and to apply it to partially straked risers. This was achieved using reliability methods, accepted industry VIV prediction software and state-of-the-art model test experiments.

Most oil companies use a Factor of Safety of 20 when predicting VIV damage using VIV software tools. There are numerous software tools currently in use in industry to predict VIV damage to straked risers and each of them will have different accuracy, and therefore an intrinsic level of conservatism. Understanding the level of conservatism in different VIV prediction software is therefore critical to determining what Factor of Safety to use.

This study benchmarks the latest generation of industry accepted VIV design tools at the time of the study (2011): SHEAR7v4.6, VIVAv6.5 and VIVANAv3.7.24 against high quality VIV data from three separate straked riser experiments. A bias distribution (predicted to measured VIV damage results) is obtained for each software tool as a function of the strake coverage.

A novel reliability framework approach is then developed to incorporate all uncertainties associated with VIV fatigue prediction into a limit state function, including variability in met-ocean conditions and variability in the fatigue resistance of the material characterized by a design S-N curve. The limit state function is analyzed using First Order Reliability Methods to develop Factors of Safety for target probabilities of failure.

The general method is then applied on two case studies involving an SCR and TTR in Gulf of Mexico loop currents, but it can be easily extended to different locations and riser configurations. The resulting FoS range from about 1 to 15 for most software, and are lower than industry standards for VIV prediction. The FoS do not vary markedly for different riser configurations, indicating the possibility of reducing excess conservatism when predicting VIV damage on straked risers.

INTRODUCTION

Understanding the level of conservatism for VIV fatigue in riser design is an important issue for operators. A significant body of research exists on developing new VIV models and improving existing ones, and benchmarking VIV software against experiments, see for example the blind predictions of laboratory measurements of VIV of a tensioned riser ([1], [2]).

Field experiments ([3], [4], [5]) and analysis of full-scale data ([6], [7], [8]) have confirmed the existence of complicating factors in VIV such as in-line vibrations, higher harmonics, intermittent behavior, travelling waves and chaotic sensitivity to small perturbations. These phenomena are only in the earliest stages of being included, if at all, in VIV fatigue analysis software.

State-of-the-art VIV fatigue design programs make the best use of available knowledge, but remain limited for the abovementioned reasons in their capacity to capture the broad complexity of VIV. In addition to more generic uncertainties with regard to structural capacity, such as variation in material properties and S-N curves, much uncertainty is linked to the amount and relevance of data available to understand and characterize VIV phenomena on full-scale risers.

To date, reported VIV fatigue damage to tubular sections of drilling risers has been minimal. Further, fatigue failures have not occurred in Steel Catenary Risers (SCR's), Top Tension Risers (TTR's) or Tension Leg Platform (TLP) tendons, indicating a high degree of design conservatism. This conservatism will have attracted significantly higher costs for deepwater riser applications.

Recognizing the industry's need to further develop an understanding of the values of FoS for VIV design, DeepStar funded a work program on VIV Factor of Safety. The work program was DeepStar Phase 10 Project 10401 for the Floating Systems Committee.

It is clear that riser VIV fatigue life estimates will always include significant, intrinsic uncertainties and approximations. There is a need to account for these in a rationally derived FoS. The objective of this work is to provide a rational basis for developing appropriate fatigue FoS for VIV and to demonstrate a benchmarking process on a high quality controlled experimental dataset.

This work presents a demonstration of the approach to determine the FoS for real configurations (SCR and TTR) based on experimental results from small to medium scale riser VIV data. The same approach would be valid in the advent of full-scale production riser VIV fatigue data. Previous attempts to calibrate VIV fatigue FOS have been made ([9], [10], [11]). The current method is developed from the limit state function formulation in [11], with the main differences being the inclusion of the riser design life and the S-N uncertainty of the riser material.

Previous work for DeepStar VIV FoS investigations [11] used NDP 38m riser model test data, as well as a basic limit state function. The new FoS results presented here are drawn from three experimental campaigns to characterize VIV response. Software has been updated since [11], and the new results are based on the most recent versions of all VIV prediction software, using default parameters. Additionally, FoS are calculated using AMOG's multiple-event limit state function, including damage from multiple currents and uncertainties in the S-N behavior of the riser material.

This work contributes to a consistent management of the risk associated with VIV by providing practical information to riser specialists regarding risk management for production risers with partial strake coverage, including consequences associated with the choice of the VIV software and the user input parameters.

NOMENCLATURE

D	Riser diameter
D^m	Actual/measured cumulative damage from VIV
D^p	Predicted total damage from VIV software
$\dot{D}_U^p(u_i)$	Predicted damage rate for current u_i
$f_U(u_i)$	Probability of current occurrence
FoS	Factor of Safety
G	Limit State Function, defining failure when $G \leq 0$
N	Number of cycles to failure found from S-N curve
P_f	Probability of failure
P_f^{ann}	Probability of failure in the last year of design life
R	Resistance variable in Limit State Function
Re	Reynolds number
S	Stress range in S-N curve (or load variable in LSF)
St	Strouhal number
T_{op}	Time of operation
U	Current magnitude
w	Proportion of total probability-weighted damage from one current profile (damage density)
α	Software bias random variable of predicted damage divided by measured damage
α_{equi}	Equivalent bias for predicted and measured damage from sum of multiple currents
Δ	Damage parameter from material S-N characteristics
σ	Scale parameter for GEV distribution
μ	Location parameter for GEV distribution
ξ	Shape parameter for GEV distribution

Methodology for developing VIV Fatigue FoS

The methodology for developing a VIV fatigue FoS draws on reliability analysis, and consists of:

- Formulating the Limit State Function (LSF) that describes the failure scenario;
- Identifying and probabilistically characterizing the uncertainties involved in the model; and
- Computing the FoS to reach a prescribed level of structural reliability.

The LSF used here is an extension of that developed in [11] and accounts for uncertainties in both the currents acting on the riser, and for the S-N behavior of the riser metal.

Reliability analysis requires characterization of the probability distributions of each of the random variables in the LSF. One random variable characterizing the software modeling error, or bias, is formulated from the ratio between measured and predicted damage for one particular current.

Datasets for this parameter are generated by systematic comparisons of predicted and measured damage for given currents from the following well-established straked riser tests:

- Miami2 152.4m (500ft) model riser tests conducted by the SHEAR7 JIP and DeepStar JIP in the Gulf of Mexico (2006) [12]. (Re=10000-75000,L/D=4200). The Miami2 experiments are described in ([13], [14] ,[15], [16])
- 38m (124.7ft) model riser tests conducted for the Norwegian Deepwater Programme (NDP) at Marintek, 2003-2004 [4]. (Re=8000-65000,L/D=1400)
- 10m (32.8ft) model riser tests conducted at Marintek for ExxonMobil, 2003 [5]. (Re=4000-50000,L/D=500).

These data sets are recognized as high quality data taken under experimental conditions, and include a large number of tests of risers with strakes, which are of significant interest due to widespread use of strakes in industry.

The software used to predict the damage for the riser cases were:

- SHEAR7 v4.6c, run by Prof. K. Vandiver;
- VIVA v6.5, run by Prof. M. Triantafyllou; and
- VIVANA v3.7.24, run by Prof. C.M. Larsen.

Default parameters were used running each program.

The final step in calibrating the FoS to desired levels of reliability is to evaluate the LSF and determine the probability of failure for multiple FoS. The First Order Reliability Method (FORM) was used, see e.g. [17]. Solving the inverse problem gives the FoS that lead to given target levels of reliability, in this case the annual probability of failure of 10^{-3}, 10^{-4} and 10^{-5} during the last year in operation.

FORMULATION OF THE LIMIT STATE FUNCTION

Background

Using reliability theory, we seek to formulate a limit state function G, such that:

$$G = R - S \tag{1}$$

where R and S describe respectively resistance of a structure and loads. Both R and S are described probabilistically using random variables. The probability of failure can be found by:

$$P_f = Pr(G \leq 0) \tag{2}$$

Failure Criterion

Failure is considered to occur when cumulative damage D^m during the time in operation T_{op} exceeds the damage parameter Δ:

$$D^m(T_{op}) \geq \Delta \tag{3}$$

where Δ reflects the large uncertainty arising from the empirical nature of the S-N model.

The annual damage rate $\dot{D}^m$ is computed by differentiating damage D^m with respect to time (exposure in years) so that the previous inequality can be rewritten in the form:

$$\Delta - \dot{D}^m \cdot T_{op} \leq 0 \tag{4}$$

where it can be seen that Δ is on the resistance side and the accumulated damage is on the loading side.

Factor of Safety

Following Leira et Al. [9], the FoS is introduced according to:

$$FoS = 1/\left(\dot{D}^p \cdot T_{op}\right) \tag{5}$$

where $\dot{D}^p$ is the annual predicted damage rate from the software.

Normalizing Eq. (4) dividing by $\dot{D}^p \cdot T_{op}$ gives:

$$\Delta/\left(\dot{D}^p \cdot T_{op}\right) \leq \dot{D}^m \cdot T_{op}/\left(\dot{D}^p \cdot T_{op}\right) \tag{6}$$

or

$$FoS \cdot \Delta \leq \frac{\dot{D}^m}{\dot{D}^p} \tag{7}$$

A convenient property of Eq. (7) is that the value of T_{op} has disappeared from the expression. It is, however, implicit in the FoS achieved by a design for a given T_{op}.

Predicted Damage and Bias Factor

The total predicted damage rate along the riser can be found by taking the damage rates predicted by VIV software for each current profile, multiplied by the current probability of occurrence:

$$\dot{D}_{TOT}(z) = \sum_i f_U(u_i) \cdot \dot{D}_U^p(u_i, z) \tag{8}$$

where $\dot{D}_U^p(u_i, z)$ is the damage predicted by the VIV software at riser position z when the riser is subjected to current profile u_i with probability of occurrence equal to $f_U(u_i)$. For analysis, $\dot{D}^p$ is taken at the riser level $z = z_{max}$ that has maximum total predicted damage:

$$\dot{D}^p = \sum_i f_U(u_i) \cdot \dot{D}_U^p(u_i, z_{max}) \tag{9}$$

The software bias is defined as the ratio of predicted damage rate per year, to measured damage rate per year, taken at a specific point on the riser:

$$\alpha = \frac{\dot{D}^p}{\dot{D}^m} \tag{10}$$

The bias is a random variable with distribution fitted to the population of the ratio of predicted to measured experimental results.

The in-situ measured damage rate $\dot{D}^m$ can be approximated by its best estimate:

$$\dot{D}^m = \sum_i \frac{1}{\alpha_i} f_U(u_i) \cdot \dot{D}_U^p(u_i) \quad (11)$$

where different (independent) random variables α_i are introduced to represent the uncertainty associated with each software prediction. $\frac{\dot{D}^m}{\dot{D}^p}$ from Eq. (7) can then be written as:

:

$$\frac{\dot{D}^m}{\dot{D}^p} = \sum_i \frac{w_i}{\alpha_i} \quad (12)$$

where each of the weights w_i is given by:

$$w_i = f_U(u_i) \cdot \dot{D}_U^p(u_i) / \sum_j \left[f_U(u_j) \cdot \dot{D}_U^p(u_j) \right] \quad (13)$$

An equivalent bias α_{equi} is then defined as a function of all weights and bias variables according to:

$$\frac{\dot{D}^m}{\dot{D}^p} = \sum_i \frac{w_i}{\alpha_i} = \frac{1}{\alpha_{equi}} \quad (14)$$

Limit State Function

The inequality describing failure during the design life T_{op} is called the Mean Time to Failure LSF, and is given by:

$$G_1 = FoS \cdot \Delta - \frac{1}{\alpha_{equi}} \quad (15)$$

with probability:

$$P_f = Pr\left[FoS \cdot \Delta - \frac{1}{\alpha_{equi}}\right] \leq 0 \quad (16)$$

It is noted that in the single current case, for example to perform a check on an isolated survival event, the single event limit state function used in previous work is recovered.

Predicted Damage and Bias Factor

The inequality describing failure before the last year of the design life is:

$$\Delta \leq \dot{D}^m (T_{op} - 1) \quad (17)$$

which can be normalized as before, to give the resulting LSF:

$$G_2 = FoS \cdot \left(\frac{T_{op}}{T_{op}-1}\right) \cdot \Delta - \frac{1}{\alpha_{equi}} \quad (18)$$

The annual failure probability in the last year of design life is:

$$P_f^{ann} = Pr[G_1 \leq 0] - Pr[G_2 \leq 0] \quad (19)$$

The direct problem involves calculating P_f^{ann} for a range of FoS. The inverse problem consists of solving for the FoS which give target levels of P_f^{ann} which can then be compared with what is specified in the design guidance.

MEASURED AND PREDICTED DAMAGE

The project used strain data collected from three experimental campaigns involving risers with different strake configurations in measured currents (both uniform and shear):

- Miami2 152.4m (500ft) model riser tests conducted by the SHEAR7 JIP and DeepStar JIP in the Gulf of Mexico (2006) [12]. (Re=10000-75000,L/D=4200)
- 38m (124.7ft) model riser tests conducted for the Norwegian Deepwater Programme (NDP) at Marintek, 2003-2004 [4]. (Re=8000-65000,L/D=1400)
- 10m (32.8ft) model riser tests conducted at Marintek for ExxonMobil, 2003 [5]. (Re=4000-50000,L/D=500).

These data from large model test basin and controlled field experiments are recognized as high quality, having been taken from rigorously designed experiments with relatively dense instrumentation arrays, and include a large number of tests of risers with strakes, which are of significant interest due to widespread use of strakes in VIV suppression.

This section describes the calculation of measured damage from the strain data obtained from the experiments, and specification of riser parameters to be used as inputs for the three VIV software programs.

Miami2 500ft DeepStar Small Reynolds Number Field Test Data

The SHEAR7 JIP (MIT) and the DeepStar JIP conducted the 2006 Gulf Stream tests ('Miami2') [12], which are described in [13], [14], [15], [16]. The experimental setup is presented in Figure 1. There were 45 partially straked cases, with 40% bottom straked, 50% staggered straked, and 50% center straked configurations as shown in Figure 2.

Each set of cases contained current data taken from an ADCP device during that test. A number of cases were rejected from further analysis, reducing the number retained for the present study to 24, due to a number of criteria, including:

- Extremely low strain response data
- Tests where hammers were used to stimulate riser response, resulting in vibrations not caused by VIV
- Other anomalous cases with very high or low response given the comparison of current input data to other tests.

The Miami2 riser data had to be pre-screened extensively as it was conducted in a variety of environmental conditions, some of which affected the validity of the data collected, as well as technical errors in the field resulting in anomalies. The original (45) cases of 40% bottom straked, 50% staggered straked, and 50% center straked riser cases were restricted to a subset of 24 cases. This selection was based on data quality issues with the rejected cases.

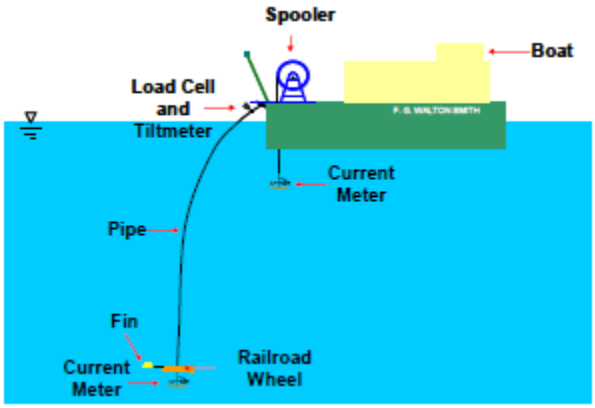

Figure 1: Experimental set-up for the Miami2 tests

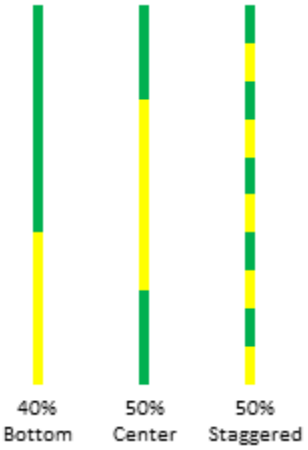

Figure 2: Strake configurations for the Miami2 tests

38m NDP Riser Data Obtained at Marintek

These experiments are detailed in [4]. A total of 121 cases were analyzed here, including both 50% straked and 100% straked configurations.

Each set of cases contains a monotonically increasing value (0.1m/s) of velocity from 0.3 to 2.4 m/s, with both shear and uniform current. As per the Marintek description [4], there are 22 different velocities in each set, except 100% straked sheared cases which have only 11.

10m Riser ExxonMobil Data Obtained at Marintek

These experiments are detailed in [5]. 120 cases were analyzed, including 25%, 50% and 75% strake configurations.

Each set of cases contains a monotonically increasing value (0.1m/s) of velocity from 0.2 to 2.38 m/s, with both shear and uniform current. There were 20 current cases for each configuration/current type pair.

Measured Damage

Measured damage was calculated from strain gauge readings at known levels down the risers. The strain time series were rainflow counted using the WAFO toolbox [18] and the DNV F2 single slope curve [19] was used to calculate an equivalent annual damage rate for each experiment. The Miami2 data set required considerable data analysis to calculate measured damage, see [12].

An important observation from the strain time series and calculation of measured damage was the presence of higher harmonics in the strain signals. All cases from the three experimental campaigns showed strong cross-flow frequency excitation at the characteristic VIV frequency:

$$f_{VIV} = \frac{St \cdot U}{D} \tag{20}$$

However, the Miami2 experiments, unlike the ExxonMobil and NDP experiments, showed significant contributions from the third and fifth harmonics ($3f_{VIV}$ and $5f_{VIV}$), particularly in the Miami2 40% bottom and 50% middle strake tests. Where higher harmonics occurred, the measured damage could be significantly higher than if the riser responded only at the first harmonic (Strouhal frequency). The measured damage was calculated with all higher harmonics included, with rainflow counting of the complete strain time series.

Predicted Damage

For each data set, predicted damage was calculated using:

- SHEAR7 v4.6c, run by Prof. K. Vandiver;
- VIVA v6.5, run by Prof. M. Triantafyllou; and
- VIVANA v3.7.24, run by Prof. C.M. Larsen.

All inputs to the VIV prediction software were selected to maximize fidelity to the experimental setup. Default values of software parameters were used for all the runs. Predicted damage was calculated at levels down the riser corresponding to sensor levels providing measured damage.

Scatterplots

Measured and predicted damage were compared for each riser experiment, at each available level, and for different software. The resulting scatterplots of measured vs. predicted damage are presented on log-log plots, see Figures 3, 4 and 5.

All analysis results indicate that the design points leading to failure scenarios are found at high measured damage. As such, the inclusion of the scatter at the lower end of the damage plot lacks relevance to the reliability of a practical fatigue damage calculation. Damage scatter plots show that the variation in the scatter for lower measured damage points was considerably larger than for higher measured damage. As such, it was determined to apply the damage threshold cutoff developed in [11] with a factor of 0.5, retaining only the upper half of all measured damage points for each strake configuration.

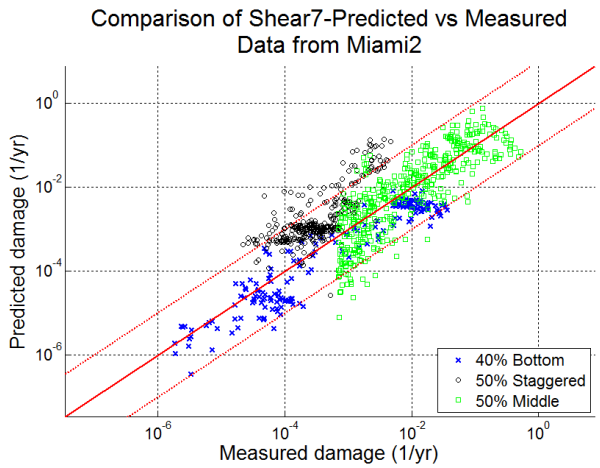

Figure 3: SHEAR7 Predicted v Measured Damage – Miami2

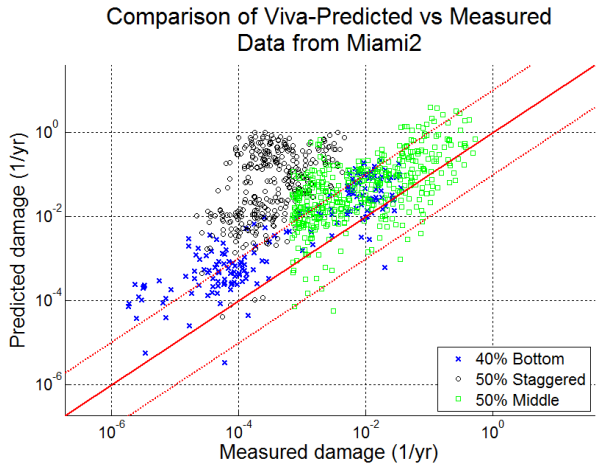

Figure 4: VIVA Predicted v Measured Damage – Miami2

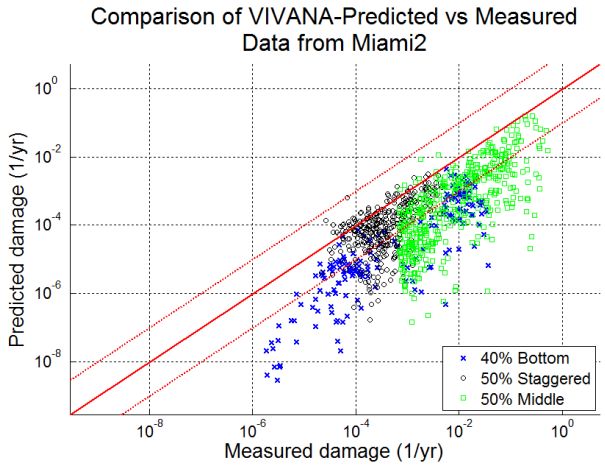

Figure 5: VIVANA Predicted v Measured Damage – Miami2

CHARACTERISING THE BIAS DISTRIBUTION

Each point on the predicted and measured damage scatter plots (Figures 3, 4 and 5) gives a unique value of α. Values of α greater than 1 correspond to scatter plot points above the line of equality, and to conservative predictions. Values of 1 indicate equality, and values below 1 are indicative of non-conservative estimates as damage is under-predicted.

The bias factor α in the LSF's of Eq. (15) and Eq. (18) is interpreted as a random variable with an associated probability distribution. The probability distribution chosen to fit α must describe the "tail" correctly, i.e. the low values of α. Low values of the bias represent VIV predictions that are under-predicted compared to experiments, and so are more likely to lead to premature failure if not properly accounted for via the FoS.

Fitting Theoretical Distributions to the Bias Indicator

To account for the long tails often evident in the observation of the bias distribution, an extreme value distribution was selected. These are distributions of the Gumbel, Frechet and Weibull types, which map maxima and minima of independently and identically distributed random variables. These distributions are very commonly used in structural engineering for finding likelihoods of events that are more extreme than any observed prior.

The generalized extreme value (GEV) distribution (also known as the Fisher-Tippett distribution) is the general form of a family that includes the asymptotic distributions mentioned above. The PDF for this three-parameter family is given by:

$$f(x) = \frac{1}{\sigma}[1 + \xi(\frac{x-\mu}{\sigma})]^{(\frac{-1}{\xi}-1)} \cdot \exp\left(-[1 + \xi(\frac{x-\mu}{\sigma})]^{\frac{-1}{\xi}}\right) \quad (21)$$

where:

- μ is a location parameter.
- σ is a scale parameter.
- ξ is a shape parameter.

The distribution type is governed by the shape parameter, ξ. The sub-families defined by $\xi = 0$, $\xi > 0$, and $\xi < 0$ correspond respectively to the extreme Gumbel, Frechet and Weibull type, i.e. distributions of extremes (maxima) from random samples following various distributions. It is important to note that μ and σ here are not equal to the mean and standard deviation of the normal distribution, though they change the shape of the distribution in a similar manner.

The Matlab function '*gevfit*' was used to fit the GEV parameters to log bias distributions for different strake cases and prediction software. An example fit is shown in Figure 6.

All distributions of the log bias were best fit with a GEV Type 3 (Weibull) distribution. This was consistent across all experiments, strake configurations, and software tools.

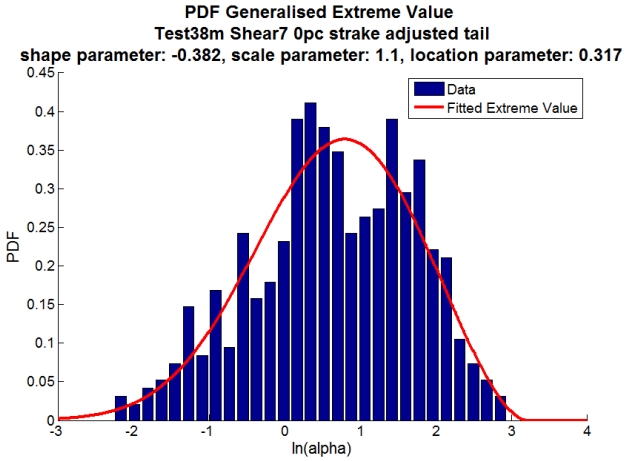

Figure 6: GEV distribution fit to log bias distribution for NDP 38m

Fitting Distribution Tail

An example CDF of the log bias from the fitted extreme Weibull distribution is shown in Figure 7. The CDF is shown with a log axis, to demonstrate the fit for small probabilities in the tail region. The distribution must fit the tail region preferentially to the body of the data, since this is where the design point occurs. The design point is the value of the random variables at which the probability of failure is calculated, being the most likely point of failure. A manual adjustment to each of the distributions was performed, changing parameters to visually optimize the fit in the tail area where the FORM design point is found, generally with CDF around 10^{-1} to 10^{-3}. The fitted Weibull extreme distribution corresponding to Figure 7 is shown in Figure 8.

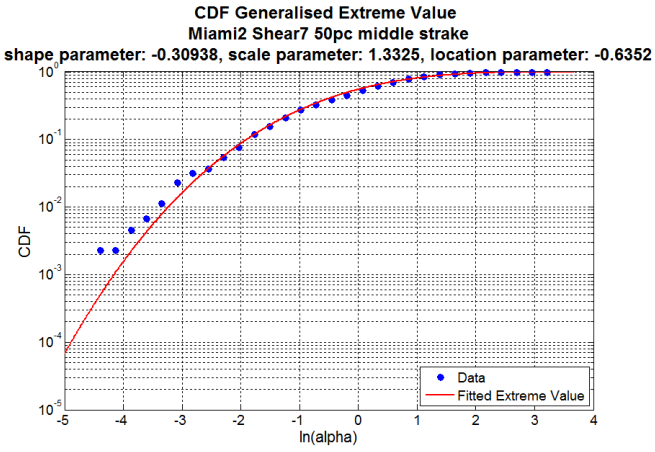

Figure 7: GEV CDF fit Miami2 riser, 50% middle strakes.

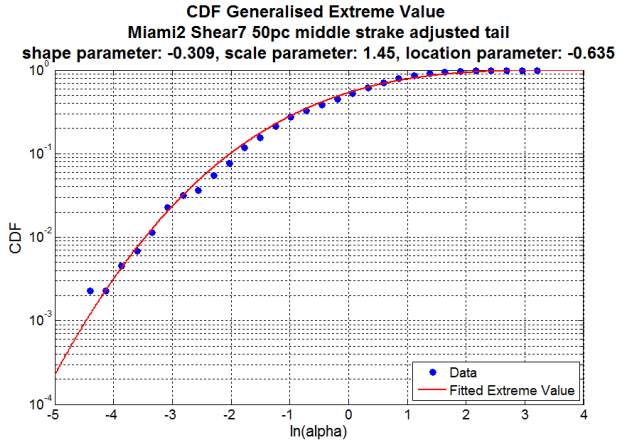

Figure 8: Adjusted GEV CDF fit Miami2 riser, 50% middle strakes.

Distributions used in the LSF

In the LSF, the adjusted tail extreme Weibull distribution is only valid in the tail of the distribution, where it is demonstrated to visibly match the experimental bias data points. The two most damaging current cases in the LSF's Eq. (15) and Eq. (18) have been assigned α_i with the adjusted tail distribution outlined here. The rest of the current cases have been assigned α_i with normal distributions fit to the whole population of log bias results. The reason for using different distributions is that the design point from FORM analysis, indicating the most likely failure point, is always found with a low value of α_i for only the highest damage current, with all other α_i near mean level. As such, only the most damaging current needs to be modeled correctly using a distribution accurate in the tail, i.e. at very low values. The remaining current cases have values of the bias variable very close to the mean at the design point.

This assumption has been checked using sensitivity analysis on the distribution types used for different currents, as well as verifying the design points from FORM where failure is calculated to occur.

FoS Numerical Computation

The procedure for calculating FoS is:

- Fit appropriate distributions to the log bias distributions.
- Find the distribution to model the damage parameter Δ (S-N strength). This is outlined in Annex A.
- Calculate the riser and current-specific weights w_i. This procedure will be outlined in the following sections, and is referred to as deterministic VIV analysis.
- Solve the two multiple event LSF's Eqs. (15) and (18) for a range of FoS using FORM, and calculate the annual failure probability P_f^{ann} from the difference.
- Interpolate the results to give the required FoS to achieve specified levels of reliability.

The multiple event LSF is solved using First Order Reliability Method (FORM). The inverse problem to find the FoS for a target reliability level is then solved by linear interpolation of the results.

The software package used to run FORM was FERUM (Finite Element and Reliability Using Matlab) v3.1 [20], an open-source uncertainty quantification toolbox for Matlab.

Results have been verified using Monte Carlo sampling and importance sampling around the design point to find the failure probability. Both these methods are significantly more time-intensive than FORM and produce varying solutions, though close agreement with FORM was found. It also provides no information about the sensitivity of the failure probability to the input parameters.

CASE STUDY: GOM SCR AND TTR

In this section, FoS for VIV fatigue are calculated for a generic 2500m SCR and 1500m TTR in 1500m water depth. Both riser models have strakes in the top 300m of their length, in the region of highest currents. Currents were selected from a scatter of GOM loop currents, including probability of occurrence, as in [21]. The calculation of FoS for these example risers is performed while quantifying all variables in the limit state function to illustrate the procedure. Conservative bounding values of the resulting FoS can be used to attain a specified level of reliability for VIV fatigue in future riser design.

Deterministic VIV Analysis for Typical SCR and TTR

The typical 2500m SCR and 1500m TTR were analyzed using the three VIV software programs, along with current cases from the scatter diagram of probability-weighted loop currents for a representative site corresponding to GOM. The current cases included 50 shear current profiles corresponding to loop currents that occur on average 71 days per year. The contribution of non-loop currents to VIV damage was neglected.

For the deterministic VIV analysis, damage rates $\dot{D}_U^p(u_i, z)$ were calculated for each current case at 1m intervals along the riser. These damage rates were multiplied by the current probability of occurrence $f_U(u_i)$ to give probability-weighted damage. The probability-weighted sum of damage from all current cases $\sum_i f_U(u_i) \cdot \dot{D}_U^p(u_i, z)$ was calculated for each riser node, and the riser level z with maximum damage selected for worst-case analysis. The 50 current profiles were ranked according to their contribution to the total probability-weighted damage at the worst-case level. The normalized damage rate corresponds to the weights w_i.

The results of the deterministic VIV analysis for SHEAR7, SCR are typical, shown in Figure 9, where the vertical axis is the value of the weights w_i corresponding to the contribution of each current case to the total probability-weighted damage at the level with highest damage. Typically, damage from the worst 3 to 4 current profiles causes about 75% of total damage.

For the purposes of FoS analysis, the top 15 weights w_{1-15} from the 15 most damaging currents were included with distinct random bias variables α_{1-15}. The remainder of the current cases, accounting for less than 10% of the damage, were lumped as one weight parameter w_{16} equal to the sum of weights of the 35 least damaging currents, and one bias variable α_{16}.

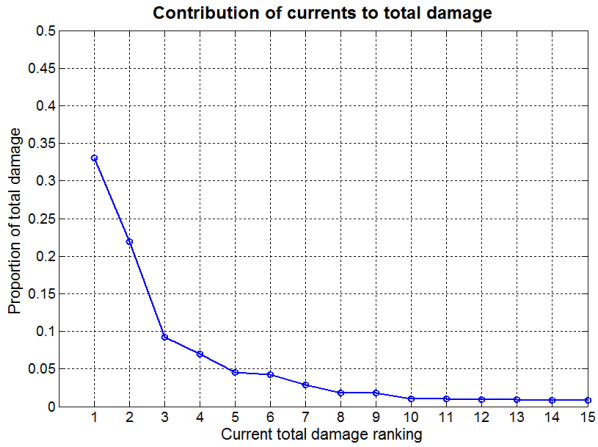

Figure 9: Proportion of total damage from 15 most damaging currents, also corresponding to first 15 weights w_i.

Annual Failure Probability

The annual probability of failure P_f^{ann} was calculated using G_1 (Eq. 15) and G_2 (Eq. 18) which respectively give the probability of failure in the design life T_{op}, taken here as 25 years, and the probability of failure before the final year. The w_i were calculated using the deterministic analysis for both risers. α_i follow distributions fitted to the predicted to measured damage results, and Δ is a log-normal distributed random variable detailed in Annex A.

Both LSF's were calculated using FORM for both the SCR and TTR, for each software tool, and for a range of FoS from 0.25 to 500. The annual failure probability P_f^{ann} decreases with increased FoS, and the relationship is non-linear.

Design Point

The design point from FORM results indicates the most likely values of all random variables in the LSF to contribute to a failure point. For each run using FORM, FERUM provides the design point in terms of the values of all random variables, including the bias random variables α_{1-16}; and damage parameter Δ.

An example of the bias variables at the design points for different P_f^{ann} is given in Figure 10. For all simulations performed, the values of the bias at the design point were characterized by:

- Bias random variable α_1 at a low, and decreasing, value ('in the tail of the distribution').
- Bias random variable α_2 at an intermediate point.
- Bias random variables α_{3-16} found very close to the mean values.

The design points indicate a failure scenario involving the most damaging current being significantly underestimated, other currents not contributing significantly, and S-N strength at a low value.

It is important to note that the value for α_1 is around $10^{-1.5}$ for $P_f^{ann} = 10^{-3}$, 10^{-2} for $P_f^{ann} = 10^{-4}$, and $10^{-2.5}$ for $P_f^{ann} = 10^{-5}$. This is because about half the contribution to a low probability failure event comes from the bias variable reaching a low value, and the other half comes from the damage parameter reaching a similar outlying level. This is important as the bias distribution will only be fitted at these low probabilities with sufficient data points. In the VIV experiments conducted, there were usually around 100-300 individual bias values fit in the distribution, and so the lowest bias value will have a CDF of 10^{-2} to $10^{-2.5}$. This means that there are only a few bias data points near the distribution fit at the low levels used to predict $P_f^{ann} = 10^{-5}$.

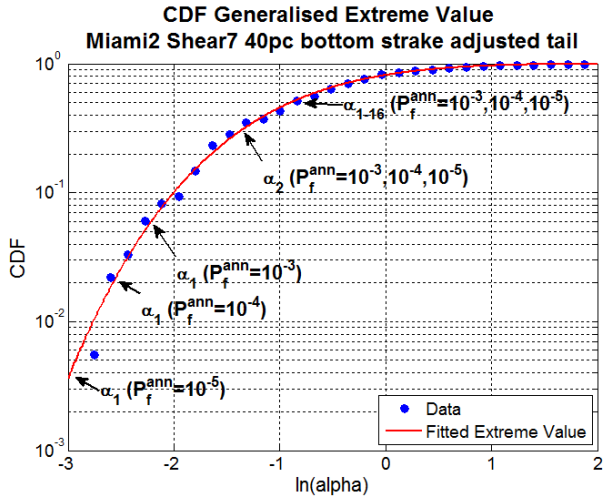

Figure 10: Design point log bias values for decreasing P_f^{ann} – SHEAR7 SCR, Miami2 40% bottom strakes

Final FoS

In the final stage of the computation, the FoS required to achieve specified targets $P_f^{ann} = 10^{-3}, 10^{-4}$ & 10^{-5} for the design SCR and TTR were interpolated from the values of P_f^{ann} calculated using FORM. A graphical interpretation of the interpolation procedure is given in Figure 11, for the TTR designed with VIVA, using bias distributions found from different Miami2 riser strake configurations.

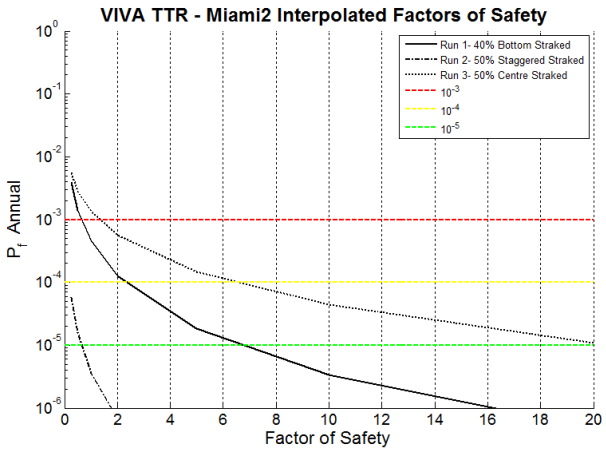

Figure 11: Interpolation of P_f^{ann} – VIVA TTR, Miami2

The upper bound FoS to achieve target levels of reliability for the SCR and TTR are given below for both SHEAR7 and VIVA:

Software & Version	Fatigue FoS for P_f^{ann} at:					
	10^{-3}		10^{-4}		10^{-5}	
	SCR	TTR	SCR	TTR	SCR	TTR
SHEAR7v4.6c	4.7	4.4	8.4	7.5	13.4	11.5
VIVA v6.5	0.8	1.3	1.4	2.4	4.0	6.8

Table 1: Summary of Bounding FoS for partially straked risers

DISCUSSION

The required FoS increases for lower target annual probability of failure (10^{-3}, 10^{-4}, 10^{-5}). Between 10% and 50% of the FoS is due to S-N uncertainty, whilst the remainder is due to VIV prediction. Even with all these uncertainties included in the analysis, the final FoS are considerably lower than those currently used in industry (~20).

The study focused on data sets from straked risers. There was considerable variation between results from different software tools, and also between different strake tests using the same software. For this reason, it has been decided that the approach most useful to riser designers is to select conservative upper bounds on the FoS values found, and use these in recommended practice.

The differences found between FoS values derived from the TTR and SCR were small, indicating the general applicability of the results across different structures. This raises the possibility of using these target FoS in the GOM for a new riser using these software tools, without re-performing reliability analysis.

A detailed study of the variability of the target FoS derived in different met-ocean conditions has not yet been conducted. The final FoS is heavily influenced by the most damaging currents. This offers the promise of accurately determining the FoS at a given site by including only the few most damaging currents.

Conversely, it is extremely important to include even low-probability currents that may cause high VIV damage, as these currents could dominate the calculation of the final FoS. As more target FoS are derived in different sites, confidence in the robustness of bounding FoS values will increase. It is expected that this will result in design levels of FoS significantly lower than the current industry standards.

Results from VIVANA were incomplete, and the deterministic VIV analysis for TTR and SCR could not be performed. Therefore, no final FoS have been calculated at this stage for VIVANA. However, the accuracy and precision of VIVANA have been investigated using VIVANA predictions for the three riser experiments conducted, giving an indication of the software performance and the likely magnitude of the FoS. For all three VIV tests, VIVANA was significantly less conservative than SHEAR7 and VIVA, often predicting much lower damage than was calculated from experimental results.
A higher FoS would be required for VIVANA than for SHEAR7 and VIVA to achieve a similar level of reliability.

Current VIV prediction software tools do not predict damage due to higher harmonics of VIV. This lack of conservatism has been included in the FoS calculated here, since the measured damage used in the bias calculation includes strain response at all frequencies.

Future work should draw on any full-scale production riser data when available to increase the confidence in the results and their applicability. Full-scale riser data would be particularly useful in clarifying the existence of higher harmonics in the VIV response. Preliminary indications from data collected on the Allegheny Steel Catenary Riser confirm the existence of higher harmonics on full-scale production risers.

CONCLUSIONS

This paper provides a detailed methodology developing a sound, reliability based Factor of Safety for tubular riser design that is quantitatively linked to target levels of reliability. The methodology can be applied during riser design as a check of the required FoS to reliably account for uncertainties in S-N behavior, met-ocean conditions and software prediction of VIV.

The FoS derived here to meet target levels of reliability are in the range 1-15, depending on software and desired level of reliability. These are significantly lower than the current industry standards of 20.

The FoS are robust to changes in riser geometry. Ongoing research by the authors suggests that similar values of FoS are found in different current profiles, including the North Sea. However, more investigation is required in different met-ocean conditions to be confident of using general FoS without performing this reliability assessment. At present, it is prudent to apply this methodology during new riser design with location and project-specific distributions of all key uncertainties.

ACKNOWLEDGMENTS

This work was funded and performed for DeepStar® Phase 10 CTR 10401 Deepwater Technology Development Project with principal contractor AMOG. Authors would like to acknowledge technical guidance and contributions of DeepStar® Floating Systems Committee chaired by Paul Devlin and a working committee of project 10401 championed by Owen Oakley, Yiannis Constantinides and Michael Tognarelli, and thank DeepStar® for permission to publish and present the results of the study.

The authors would like to acknowledge the NDP (Norwegian Deepwater Program) for the use of the 38m riser data. ExxonMobil is acknowledged for the contribution of the 10m riser data. The DeepStar® JIP previous Phases 7 & 8 as well as contributions from the SHEAR7 JIP are acknowledged for use of the Miami2 data. The VIVDR (Vortex-Induced Vibration Data Repository) a product of OMAE symposia for VIV and CFD, and currently hosted by MIT, is acknowledged for hosting the publicly available VIV data.

REFERENCES

[1] Chaplin, Bearman, Cheng, Fontaine, Graham, Herfjord, Huera-Huarte, Isherwood, Lambrakos, Larsen, Meneghini, Moe, Pattenden, Triantafyllou, Willden (2005) "Blind predictions of laboratory measurements of vortex-induced vibrations of a tension riser", Journal of Fluids and Structures, Vol. 21, pp. 25-40

[2] Bearman, Chaplin, Fontaine, Graham, Herfjord, Huera-Huarte, Lima, Meneghini, Schulz, Willden (2006) "Comparison of CFD Predictions of Multi-Mode Vortex-Induced Vibrations of A Tension Riser with Laboratory Measurements", Proc. 6th Intern. Symposium on FSI, AE & FIV: ASME PVP Division Summer Meeting, Vancouver, BC, Canada, July 23-27

[3] Marcollo, Vandiver & Chaurasia (2007), "Phenomena Observed in VIV Bare Riser Field Tests", 26th International Conference on Offshore Mechanics and Arctic Engineering, OMAE2007-29562

[4] Norwegian Marine Technology Research Institute (Marintek), "NDP Riser High Mode VIV Tests – Main Report", Report No: 512394/Main report ver02 (draft), 24th March 2004. Publicly available at oe.mit.edu/VIV

[5] Norwegian Marine Technology Research Institute (Marintek), "VIV Suppression Test on High L/D Flexible Cylinders – Main Report", Report No: 512382.00.01 draft, 15th July 2003. Publicly available at oe.mit.edu/VIV

[6] Trim, Braaten, Lie, Tognarelli (2005), "Experimental investigation of vortex-induced vibration of long marine risers", Journal of Fluids and Structures

[7] Tognarelli, Taggart, Campbell (2008) "Actual VIV Fatigue Response of Full Scale Drilling Risers: With and Without Suppression Devices", 27th International Conference on Offshore Mechanics and Arctic Engineering, OMAE2008-57046

[8] Vandiver, Swithenbank, Jaiswal & Marcollo (2006), "The Effectiveness of Helical Strakes in the Suppression of High-Mode Number VIV", Offshore Technology Conference, OTC 18276. Winner of IPTI – LUBINSKI Best Paper Award

[9] Leira, Meling, Larsen, Berntsen, Stahl & Trim (2005) "Assessment of Fatigue Safety Factors for Deep-Water Risers in Relation to VIV", Journal of Offshore Mechanics and Arctic Engineering, Nov 2005, Vol. 127 pp353-358

[10] Tognarelli, Fontaine, Beynet, Santosa, Marcollo (2010), "Reliability-Based Factors of Safety for VIV Fatigue Using Field Measurements" Proc. 29th Int'l Conf. Ocean, Offshore & Arctic Engineering, ASME, OMAE2010-21001

[11] Fontaine, Marcollo, Vandiver, Triantafyllou, Larsen, Tognarelli, Constantinides, Oakley (2011), "Reliability Based Factors of Safety For VIV Fatigue Using NDP Riser High Mode VIV Tests", Proc. 30th Int'l Conf. Ocean, Offshore & Arctic Engineering, ASME, OMAE2011-49820

[12] DeepStar VIII Project, (2007), "DeepStar 8402: Gulf Stream Experiment October 2006", Document No.: DSVIII CTR 8402.

[13] Jaiswal, V. and Vandiver, J.K., 2007, "VIV Response Prediction for Long Risers with Variable Damping", Proceedings of OMAE2007, OMAE2007-29353

[14] Jhingran, V. and Vandiver, J.K., 2007, "Incorporating the Higher Harmonics in VIV Fatigue Predictions", Proceedings of OMAE2007, OMAE2007-29352

[15] Marcollo, H., Chaurasia H. and Vandiver J. K., "Phenomena Observed in VIV Bare Riser Field Tests", Proceedings of OMAE2007, OMAE2007-29562

[16] Swithenbank, S. and Vandiver, J.K., 2007, "Identifying the Power-in Region for Vortex-Induced Vibration on Long Flexible Cylinders", Proceedings of OMAE2007, OMAE2007- 29156

[17] Melchers R. E. (1987) "Structural reliability analysis and prediction", Ellis Horwood Series, John Wiley & Sons Ltd.

[18] Wave Analysis for Fatigue and Oceanography. Homepage, Lund Institute of Technology, March 2007, http://www.maths.lth.se/matstat/wafo/

[19] DNV, "Fatigue Strength Analysis for Mobile Offshore Units" Classification Notes, Note No. 30.2, August 1984

[20] Finite Element Reliability Using Matlab, UC Berkeley, (FERUM), v3.1, Homepage, http://www.ce.berkeley.edu/projects/ferum/index.html

[21] Aker Kvaerner, "Disconnectable FPSO with Hybrid Riser System for Ultra-Deep Waters in the GOM" Doc Reference 102399-AKI-RA-Z-0001 Revision A, 2008

ANNEX A

The limit state function includes the damage parameter Δ as a random variable. The objective of this section is to characterise the distribution of the damage parameter. As Δ is a measure of the value of the damage at failure, there is a theoretical link between the distribution of the damage parameter and the uncertainty associated with S-N curves.

Melchers [17], Section 6.8 "Fatigue analysis" describes the reliability framework for modelling S-N behaviour:

"The traditional model to describe the fatigue life N_i of a component or structure under constant-amplitude repeated loading is given by, for example, the American Society of Civil engineers (ASCE) (1982)

$$N_i = K/S_i^m \tag{22}$$

where K and m are conventionally taken as constants, but as random variables here, and N_i is the number of stress cycles at constant stress amplitude S_i. Test results normally allow m and K to be estimated. Typically, conservative values are used such that Eq. (22) produces a safe estimate of fatigue life. For a reliability analysis, the model given by Eq. (22) must be a realistic rather than a conservative predictor, so that typical values for m and K quoted in the literature may not be appropriate…

In practice the amplitude of the stress cycles is not constant but is a random variable. If the number of cycles which occur at each amplitude level can be measured or estimated, the empirical Palmgren-Miner hypothesis

$$\sum_{i=1}^{N} \frac{n_i}{N_i} = \Delta \tag{23}$$

is often adopted. Here n_i represents the actual number of cycles at the stress amplitude S_i. If the stress amplitudes are all different, then:

$$\sum_{i=1}^{N} \frac{1}{N_i} = \sum_{i=1}^{N} K^{-1} S_i^m = \Delta \tag{24}$$

where N is the total number of (random) variable-amplitude cycles. The damage parameter Δ is conventionally taken as unity but may typically lie in the range 0.9-1.5. Hence Δ reflects the (large) uncertainty arising from the empirical nature of Eq. (22). A lognormal distribution with unit mean and a coefficient of variation of about 0.4-0.7 appears appropriate [Madsen, 1982; ASCE, 1982]."

The damage $\dot{D}^p$ and $\dot{D}^m$ have been calculated using the DNV F2 Class design S-N curve [19] for air, which is identical to seawater with cathodic protection, but without an endurance cutoff. This is based on statistical analyses of appropriate experimental data and provides the linear relationship between $log\,(S)$ and $log\,(\bar{N})$ in the form

$$\log(\bar{N}) = \log(\bar{a}) - m log(S) \tag{25}$$

or

$$\bar{N} = \bar{a}/S^m \tag{26}$$

where:

- $\bar{N}$ is the conservative number of cycles to failure under stress range;
- $\bar{a}$ is a constant relating to the mean S-N curve minus two standard deviations;
- m is the inverse slope of the S-N curve for Class F2; and
- log is the logarithm with base 10.

The constant $\bar{a}$ in Eq. (25) is given by

$$\log(\bar{a}) = \log(a) - 2log(s) \tag{27}$$

where:

- $\log\,(a)$ is the mean value observed during numerous experiments; and
- $\log\,(s)$ is the value of the standard deviation of $\log\,(N)$ observed during the experiments.

$\log(\bar{a}) = 11.63$ and $\log(s) = 0.2279$ for DNV F2 Class.

The mean-valued DNV F2 S-N curve is given by

$$N = a/S^m \tag{28}$$

where $\log(a) = 12.09$.

Figure A1 shows a comparison of the design S-N curve in red, and the mean S-N curve in black, with 100 random points following the distribution with mean $\log(a) = 12.09$ and with standard deviation for DNV F2 Class: $\log(s) = 0.2279$. As can be seen, the design S-N curve is significantly conservative.

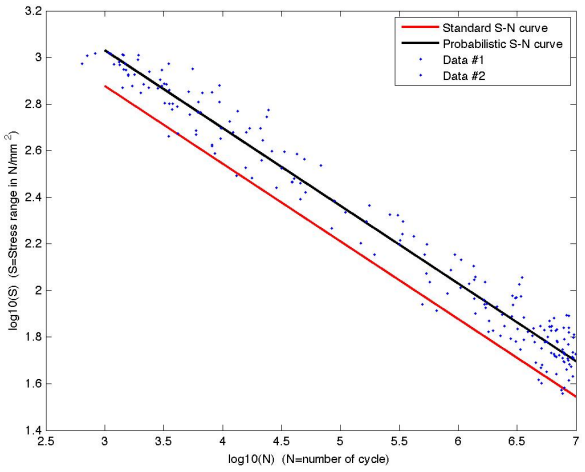

Figure A1: Class F2 S-N curves. Comparison between the "true" and codified S-N curves.

To find the damage parameter distribution, firstly, the true number of cycles N' to failure is given as a random variable:

$$N' = a'/S^m \tag{29}$$

where a' is a random variable with mean value equal to a and distribution given by

$$a' = 10^{(N(\mu=\log(a),\sigma=\log(s)))} \tag{30}$$

where the notation $N(\mu,\sigma)$ is used to represent a Gaussian distribution with mean value μ and standard deviation σ.

The true total damage from variable amplitude loading is calculated using the Miner-Palmgren rule, i.e. summing each of the individual damage d_i according to:

$$D_{TRUE} = \sum d_i = \sum \frac{n_i}{N_i'} \tag{31}$$

where n is the number of cycles in the stress range S_i and N_i' is the number of cycles to failure for that stress range. The limiting value of damage is 1.

However, when the damage is calculated using the conservative $\bar{N}$ from the design F2 Class S-N curve, as is the case with the measured and predicted damage, the total damage will follow:

$$D = \sum d_i = \sum \frac{n_i}{\bar{N}_i} \tag{32}$$

The value of D in terms of D_{TRUE} is equal to

$$D = \sum \frac{n_i}{N_i'} \cdot \frac{N_i'}{\bar{N}_i} = D_{TRUE} \cdot \frac{N_i'}{\bar{N}_i} \tag{33}$$

Since the value of D_{TRUE} at failure is 1 (by the definition of Miner's Rule), the value of the damage predicted using the conservative S-N curve at failure (Δ) is equal to

$$\Delta = 1 \cdot \frac{N_i'}{\bar{N}_i} \tag{34}$$

$\frac{N_i'}{\bar{N}_i}$ is constant between all stress states i, for a given realization of the S-N curve.

$$\frac{N_i'}{\bar{N}_i} = \frac{a'}{\bar{a}} = 10^{(N(\mu=\log(a)-\log(\bar{a}),\sigma=\log(s)))} \tag{35}$$

giving

$$\Delta = 10^X \tag{36}$$

where

$$X \sim N(\mu = 2\log(s), \sigma = \log(s)) \tag{37}$$